Hall, A., & Knowles, J. R. (1975) *Biochemistry 14*, 4348–4352.

Hartman, F. C. (1970) *Biochem. Biophys. Res. Commun. 39*, 384–388.

Hol, W. G. J., van Duijnen, P. T., & Berendson, H. J. C. (1978) *Nature (London) 273*, 443–446.

Joseph, D., Petsko, G. A., & Karplus, M. (1990) *Science 249*, 1425–1428.

Kemp, D. S., Cox, D. D., & Paul, K. G. (1975) *J. Am. Chem. Soc. 97*, 7312–7318.

Komives, E. A., Chang, L. C., Lolis, E., Tilton, R. F., Petsko, G. A., & Knowles, J. R. (1991) *Biochemistry 30*, 3011–3019.

Lolis, E., & Petsko, G. A. (1990) *Biochemistry 29*, 6619–6625.

Lolis, E., Alber, T. C., Davenport, R. C., Rose, D., Hartman, F. C., & Petsko, G. A. (1990) *Biochemistry 29*, 6609–6618.

Nickbarg, E. B., Davenport, R. C., Petsko, G. A., & Knowles,

J. R. (1988) *Biochemistry 27*, 5948–5960.

Petsko, G. A., Davenport, R. C., Frankel, D., & RajBhandary, U. L. (1984) *Biochem. Soc. Trans. 12*, 229–232.

Pompliano, D. L., Peyman, A., & Knowles, J. R. (1990) *Biochemistry 29*, 3186–3194.

Rebek, J., Jr. (1990) *Angew. Chem., Int. Ed. Engl. 29*, 245–255.

Richard, J. P. (1984) *J. Am. Chem. Soc. 106*, 4926–4936.

Rieder, S. V., & Rose, I. A. (1959) *J. Biol. Chem. 234*, 1007–1010.

Rose, I. A. (1982) *Methods Enzymol. 87*, 84–97.

Straus, D., Raines, R. Kawashima, E., Knowles, J. R., & Gilbert, W. (1985) *Proc. Natl. Acad. Sci. U.S.A. 82*, 2272–2276.

Tidor, B., & Karplus, M. (1991) *Biochemistry 30*, 3217–3228.

Waley, S. G., Mill, J. C., Rose, I. A., & O'Connell, E. L. (1970) *Nature (London) 227*, 181.

Computer Simulation and Analysis of the Reaction Pathway of Triosephosphate Isomerase[†]

P. A. Bash,[‡,§] M. J. Field,[‡,‖] R. C. Davenport,[⊥,○] G. A. Petsko,[⊥,#] D. Ringe,[⊥,#] and M. Karplus[*,‡]

Department of Chemistry, Harvard University, Cambridge, Massachusetts 02138, and Department of Chemistry, Massachusetts Institute of Technology, Cambridge, Massachusetts 02139

Received February 12, 1991; Revised Manuscript Received March 22, 1991

ABSTRACT: A theoretical approach designed for chemical reactions in the condensed phase is used to determine the energy along the reaction path of the enzyme triosephosphate isomerase. The calculations address the role of the enzyme in lowering the barrier to reaction and provide a decomposition into specific residue contributions. The results suggest that, although Lys-12 is most important, many other residues within 16 Å of the substrate contribute and that histidine-95 as the imidazole/imidazolate pair could act as an acid/base catalyst.

Although there have been many discussions of the factors contributing to rate enhancement by enzymes (Fersht, 1985; Jencks, 1975, 1987; Kraut, 1988), our understanding is limited by the lack of detailed information at the molecular level. An enzyme that has been the subject of intensive experimental studies is triosephosphate isomerase (TIM). TIM catalyzes the interconversion of dihydroxyacetone phosphate (DHAP) and D-glyceraldehyde 3-phosphate (GAP), an essential step

in the glycolytic pathway. The TIM-catalyzed reaction is 9 orders of magnitude faster than that catalyzed by acetate ion in aqueous solution (Hall & Knowles, 1975; Richard, 1984). Although a wide range of experiments, including kinetics (Rose, 1962; Herlihy et al., 1976; Albery & Knowles, 1976b), X-ray crystallography (Banner et al., 1975; Alber et al., 1981; Davenport et al., 1991), NMR (Browne et al., 1976) and infrared (Belasco & Knowles, 1980) spectroscopy, and site-specific mutagenesis (Nickbarg et al., 1988), have been applied to TIM, the role of the enzyme in determining the energetics along the reaction path is not fully understood. Glu-165 has been implicated as the catalytic base (Rose, 1962; Herlihy et al., 1976; Hartman, 1970; Waley et al., 1970; de la Mare et al., 1972; Banner et al., 1975; Alber et al., 1981), and a recent crystallographic study (Davenport et al., 1991), together with site-specific mutagenesis (His-95 → Gln) (Nickbarg et al., 1988; Komives et al., 1991), suggests that His-95 also plays an important role in the enzymatic reaction.

To obtain a more detailed knowledge of the mechanism of TIM, theoretical approaches of the type now being widely applied to macromolecules of biological interest (Brooks et al., 1988; Karplus & Petsko, 1990) can be used to supplement the available experimental data. We report a calculation of the TIM reaction path that employs a simulation method (Field et al., 1990) developed for the study of reactions in solution
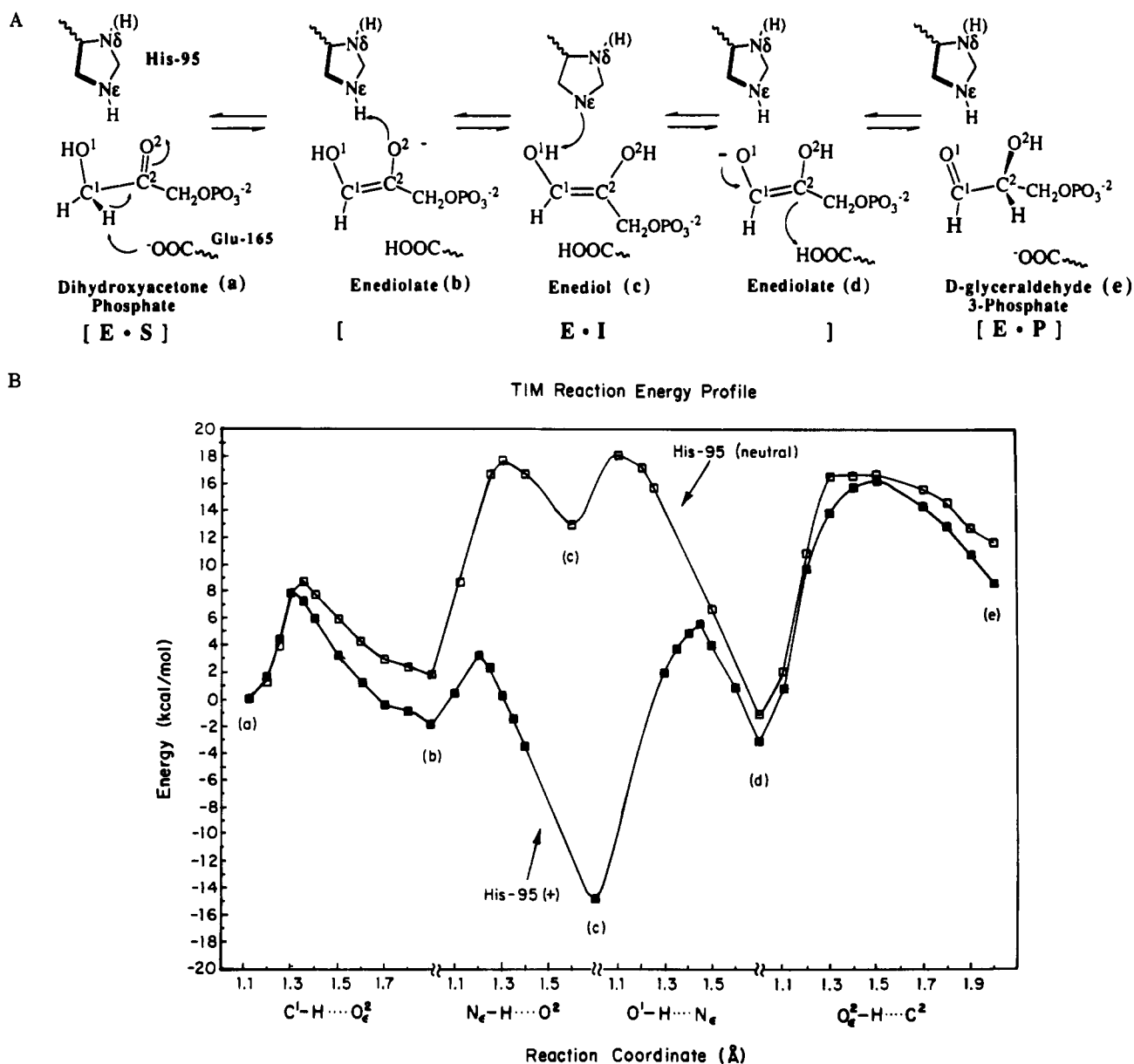
FIGURE 1: (A) Putative mechanism for the isomerization of dihydroxyacetone phosphate (DHAP) to D-glyceraldehyde 3-phosphate (GAP) with residues Glu-165 and His-95 of TIM acting as acid/base catalysts. (B) Energy profile for the proton transfer steps depicted in (A). The ordinate is $E_{QM/MM}$ normalized to the ground-state energy for the enzyme–substrate complex. The reaction coordinates for the various steps shown in (A) are indicated along the abscissa; for each step the distance measures that of the transferred proton from the heavy atom to which it is bonded in the reactant.

or in an enzyme. Figure 1A shows the steps of the reaction catalyzed by TIM. They proceed from the enzyme–substrate complex to the enzyme–product complex; the pathway shown is a somewhat more detailed version of the chemical transformation steps considered previously (Albery & Knowles, 1976a,b; Knowles & Albery, 1977).

Since theoretical approaches are valid only if based on accurate structural data, we make use of the recent high-resolution X-ray structure of yeast TIM inhibited by phosphoglycolohydroxamate (PGH), an intermediate analogue (Davenport et al., 1991). The X-ray structure indicates that (i) Glu-165 and His-95 are positioned to facilitate the proton transfers depicted in Figure 1A, (ii) Asn-10 and Lys-12 are positioned to stabilize reaction intermediates, and (iii) His-95 is singly protonated at Nε. The simulations demonstrate that, although the proximity of the carboxylate of Glu-165 to the methylene group of DHAP is necessary for the first step of proton transfer (a → b in Figure 1A), it is not sufficient. Other amino acids are involved in determining the barrier and the

relative energy of the reactants and the enediolate intermediate; the most important of these are conserved in 12 (out of 13) TIM sequences[1] (Lolis et al., 1990) and some are as far as 16 Å from the catalytic site. In addition, we address the issue of the protonation state of His-95 and its role in the reaction mechanism. Although it is generally thought that the imidazole of histidine must be doubly protonated to act as an acid, the simulation suggests that neutral imidazole can transfer a proton to O2 of the enediolate. The final proton transfer from the neutral Glu-165 to C2 has characteristics similar to the initial methylene proton transfer step. Overall, the computer simulation and its analysis demonstrate at an atomic level of detail how this "perfect" enzyme can lower the reaction barrier without overstabilizing the intermediates, in accord with the

---

[1] The single exception is *Bacillus stearothermophilus*, where a protein sequence but no X-ray structure is known. In this species, residue 237 is a Glu instead of the Lys found in yeast TIM, and residue 214 is a Lys instead of an Asn, which is within 5 Å of Lys-237 in yeast TIM.

formulation of Knowles and Albery (1977).

EXPERIMENTAL PROCEDURES

The theoretical method used here combines quantum and molecular mechanics techniques to provide a general formulation for the study of condensed phase reactions (Field et al., 1990). The present approach is similar in concept to, but different in implementation from, methods introduced previously (Wang & Karplus, 1973; Warshel & Levitt, 1976; Singh & Kollman, 1986). To describe changes in the electronic structure of the reacting species (bond making and bond breaking), a semiempirical quantum mechanical (QM) method (Austin Model 1, AM1; Dewar & Thiel, 1977; Dewar et al., 1985) is used for the subset of atoms directly involved in the reaction. The remainder of the system (other protein atoms and/or solvent) is treated by molecular mechanics (MM) (Brooks et al., 1983), and the two subsystems are coupled by electrostatic and van der Waals interactions. The energies ($E_{QM/MM}$) of and the forces ($F_{QM/MM}$) on the QM atoms are given by the expectation value of the QM Hamiltonian and its derivative, respectively, and include electrostatic and van der Waals interactions with the MM atoms. Knowledge of $F_{QM/MM}$ and F_{MM}, the forces on the MM atoms (which include contributions from the QM atoms), permits energy minimization and classical molecular dynamics to be done in a standard manner (Brooks et al., 1983; Field et al., 1990). The energy $E_{QM/MM}$ is used for analysis of the results because it is the dominant term for the reaction considered in the present calculations. The proton transfers in TIM create small local changes in the electron distribution and structure, which will be mostly accounted for in $E_{QM/MM}$; the remainder, E_{MM}, should be an essentially constant background. Moreover, for primarily electrostatic interactions, such as those considered here, the free energy is directly related to the interaction energy (Roux et al., 1990). Details of the method together with an extensive series of tests on model systems are presented elsewhere (Field et al., 1990); a study of the S_N2 reaction (Cl$^-$ + CH_3Cl) in aqueous solution has demonstrated the applicability of the method for determining the effects of solvation along a reaction path (Bash et al., 1987).

Initial atomic coordinates for the simulations were obtained from the refined X-ray crystal structure of the TIM-PGH complex (Davenport et al., 1991), with the amide NH group of the PGH replaced by a CH_2 methylene group in a tetrahedral configuration to form the DHAP substrate. A 16-Å spherical region centered on atom $O\epsilon2$ of Glu-165 was selected as the model system for the simulations. Explicit water molecules were introduced to solvate the active site of the enzyme, and stochastic boundary conditions were applied as described previously (Brooks & Karplus, 1989). The stochastic boundary system based on the X-ray structure was energy minimized by using the QM/MM hybrid method with the substrate and the side chains of Glu-165 and His-95 treated quantum mechanically and all other atoms described by a molecular mechanics potential (Brooks et al., 1983). This provided the reference energy and starting structure for subsequent simulations. The simulation system consisted of 1250 protein atoms and 100 water molecules. We report results for only one of the active sites; all calculated values for the other active site are very similar. Minimizations were done without a nonbonded cutoff until a root-mean-square (rms) gradient of less than 0.01 kcal/Å and a change in energy over the last 100 steps of less than 0.02 kcal/mol were achieved. This required on the order of 2000 steps. Each pathway was determined by first restraining the transferring proton to be equidistant between the donor and acceptor atoms by adding

a harmonic constraint ($k = 10^4$ kcal/Å^2 with a distance of 1.4 Å between the hydrogen and the two heavy atoms) while minimizing the entire structure for 250 steps. After this initial minimization, the constraint between the proton and acceptor atom was removed and the distance between the hydrogen and donor atom was varied to map out the energy profile for the transfer of the proton between the two heavy atoms. To minimize potential drift in energy along this pathway, each point was determined by starting from the initial minimized structure with the proton equidistant from the donor and acceptor and the same number of steps (250) of minimization was used.

To verify that the simulation system is well behaved, the reference structure (see above) was compared with the original TIM-PGH X-ray structure. The root-mean-square deviation between this structure and the X-ray coordinates was 0.504 Å (0.636 Å) for main-chain (all) protein atoms included in the system. This is comparable to the rms difference of 0.39 Å for the $C\alpha$ atoms of the two monomers [see Davenport et al. (1991)]. More important, the relative positions of key groups (His-95, Glu-165, Lys-12, and DHAP) after the minimization are very similar to those in the TIM-PGH X-ray structure. We give some of the distances (in angstroms) between atoms in the active site that are involved in the reaction; values from the X-ray structure and after the minimization are shown. Nϵ (His-95)-O1 = 3.1/3.0, Nϵ (His-95)-O2 = 2.7/2.9, Nζ(Lys-12)-O2 = 2.8/2.79, Nδ(His-95)-N(Glu-97) = 2.8/3.1, and Oϵ2(Glu-165)-N(PGH) = 2.7/Oϵ2(Glu-165)-Cl(DHAP) = 3.0. These differences are similar to those between the independently refined active sites in the two monomers; e.g., for site 1/site 2, Nϵ-O1 = 3.1/2.9, Nϵ-O2 = 2.7/2.8, Nζ(Lys-12)-O2 = 2.8/2.8, O(Glu-165)-N(PGH) = 2.7/2.7. Also, in accord with the X-ray structure, the carboxyl of Glu-165 is in position to abstract the *pro-R* proton from the Cl of DHAP with the syn orbital of Oϵ2 in close proximity to this proton [see Figure 3 of Davenport et al. (1991)], and His 95 Nϵ is located between O1 and O2 of DHAP.

RESULTS

It is known that the AM1 method used for the QM subsystem is about 1000 times faster (Dewar & Storch, 1985) than ab initio techniques (Hehre et al., 1986) and that it yields satisfactory results for many properties of organic molecules, such as ground-state and transition-state geometries and proton affinities (Dewar et al., 1985; Dewar & Dieter, 1986; Schroeder & Thiel, 1985). However, as shown in test calculations (Field et al., 1990), the errors can be significant in some cases, so that it is important to compare the semiempirical results with experiment and high-level ab initio calculations for analogues of the molecules or fragments of interest. Table I gives a comparison of deprotonation energies (DPE) for the key chemical groups involved in the scheme shown in Figure 1A. The AM1 values compare well with experiment and with high-level ab initio calculations; the largest AM1 deviation from experiment is 1.6% (5.6 kcal for reaction E), comparable to the experimental uncertainty of 2–4 kcal. This test indicates that application of the methodology to the TIM reaction should permit meaningful, albeit only semiquantitative, statements concerning the mechanism.

The reaction profile for the steps depicted in Figure 1A is shown in Figure 1B, which presents the results with His-95 initially singly or doubly protonated. For the first step (a → b in Figure 1A), the distance between Oϵ2 of Glu-165 and Cl of CH_2 of DHAP in the minimized structures is in the range 2.6–3.3 Å during the transfer. This result is in accord with

A

Center of Mass Distance (Å)

B

Energy Difference : Enediol · Enediolate
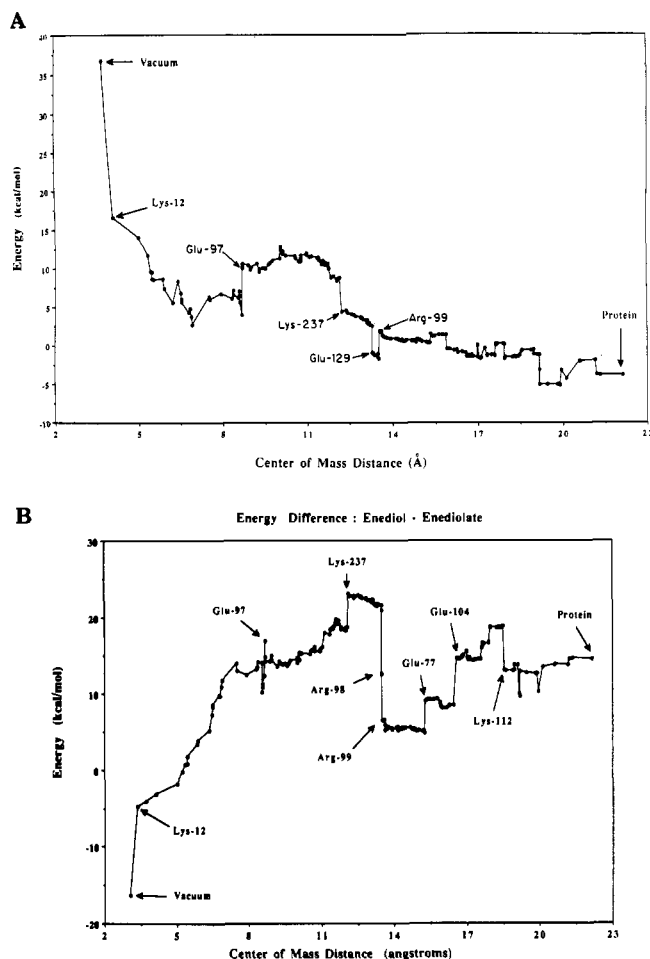

Center of Mass Distance (angstroms)

FIGURE 2: First-order perturbation estimate of residue contributions to the energy along reaction pathway. (A) Plot of the $E_{QM/MM}$ energy difference (due to electrostatic potential of specific residues) between states (b) and (a) of Figure 1A as a function of the fraction of the protein included in the calculations. The abscissa represents an ordering of amino acid residues by the distance from their center of mass (COM) to that of the substrate. The points on the curve were obtained by setting the MM charges to zero on residues in order from the furthest to the closest COM distance. His-95 is in a singly protonated state for these calculations. (B) The same as (A) for states (c) and (b) of Figure 1A. "Vacuum" in the figure refers to the energy difference calculated when the charges on all amino acids, other than those treated as QM atoms, were set to zero.

the model compound calculations of Alagona et al. (1984), who showed the barrier is very sensitive to the donor–acceptor distance; they also pointed out the importance of Lys-12. Interestingly, His-95 in the neutral state has only a small (≈ 3

kcal/mol) effect on the transition-state energy for this step; the effect of a protonated His is only slightly larger due to its delocalized charge distribution.
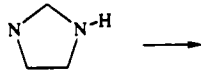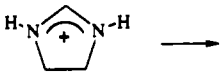
The transfer of the proton from O2 to O1 of the enediolate (b → d in Figure 1A) is thought to involve His-95 either as an electrostatic catalyst or as a generalized base and acid (Hartman, 1970). The present calculations (see Figure 1B) suggest that the Nε of a neutral His-95 can transfer a proton to O2 of the enediolate to form the imidazolate and an enediol with an energy barrier for the proton transfer on the order of the experimental estimate (≈ 13 kcal) (Albery & Knowles, 1976b). A corresponding calculation has been made for doubly protonated His-95. When this simulation is carried out, His-95 reorients from its position in the crystal structure (Davenport et al., 1991) so as to move its Nδ hydrogen away from the amide hydrogen of residue 97. This leads to a very different reaction profile with a deep well for the state involving the enediol and neutral histidine (Figure 1B). There is no evidence for such a stable enediol intermediate (Albery & Knowles, 1976b), whose existence would hinder the reaction. Neither the structural data nor the calculations can exclude the possibility that a transiently formed protonated His-95 is the catalytic acid, nor that a concerted proton transfer between substrate oxygens occurs via neutral His as a relay, but they do suggest the novel possibility that a neutral His-95 could be effective as the generalized acid. The second pK_a of His (His → His⁻ + H⁺) is about 14 in aqueous solution (Yegil, 1967). Although the conditions in the enzyme are different from those in solution, this suggests the possibility of a balance between the pK_a's of a neutral His and the enediol; the pK_a of an enediol has not been measured, but values for enols are in the neighborhood of 11 (Haspra et al., 1979). This contrasts with the apparent imbalance between the pK_a of a protonated His and the enediol, which the calculations indicate results in a thermodynamic "trap" for the intermediate.

By use of a perturbation technique (see caption of Figure 2), the effects of individual amino acids on the energy difference between Glu⁻ + DHAP and GluH + enediolate (Figure 2A, a → b in Figure 1A) and that between enediolate + His and enediol + His⁻ (Figure 2B; b → c in Figure 1A) were determined. Many of the same residues are important for the reaction involving protonated His-95. Figure 3 shows the location of some of the important residues. Lys-12 has the largest effect on both steps in the catalyzed reaction. The protonated amino group of Lys-12 is close to O2 of the inhibitor in the TIM–PGH crystal structure and remains there during the simulations of the reactions (Nζ of Lys-12 to O2 is 3.0–3.1 Å for neutral His and 3.1–3.4 Å for His⁺). The

FIGURE 3: Stereoview of some important charged residues that contribute. The Cα backbone is shown as a light black line, and the side chains of the residues of interest are shown by heavy black lines.

Table I: Deprotonation Energies for Compounds Related to the Groups Directly Involved in the Enzyme Reaction[d]

		Expt	AM1	6-31+G*	MP2/6-31+G*
A	(imidazole → imidazolide reaction)	352.0[a]	347.6	360.4	349.4
B	(protonated imidazolium → imidazole reaction)	222.1[b]	221.9	236.2	228.0
C	(pyrrole N-H → pyrrolide reaction)	360.8[c]	355.4	370.7	360.1
D	(CH(OH)–CO–CH₃ → C(OH)=C(O⁻)–CH₃ reaction)	-	367.1	382.7	367.3
E	(CH_3CH_2-COOH → $CH_3CH_2-COO^-$ reaction)	347.3[c]	352.9	355.9	345.6
F	(C(OH)H–C(OH)–CH₃ → C(OH)=C(O⁻)–CH₃ reaction)	-	357.4	360.4	351.7

[a] Meot-Ner (1988). [b] Pearson (1986). [c] Dewar and Dieter (1986). [d] A, B, and C give an indication of the accuracy of the calculations of proton transfers facilitated by His-95. D and E are related to the methylene proton transfer, and F gives the affinity of a proton for an enediolate. For the ab initio calculations each molecule was optimized by using a 6-31+G* basis set and the Gaussian 86 program (1986). The resultant geometries were then used to determine single point energies by using a 6-31+G* basis set and Moller–Plesset perturbation theory to second order (MP2).

protonated amino group stabilizes the enediolate by 20.1 kcal/mol (b in Figure 1A) relative to DHAP (a in Figure 1A) because O2 is more negative after removal of the methylene proton (the Mulliken charges are −0.32 and −0.65, respectively). On the other hand, the protonated O2 (c and d in Figure 1A) is less negative than the ionized O2 (b in Figure 1A) so that there is a destabilizing interaction of 11.5 kcal with Lys-12 in the transfer step (b → c in Figure 1A). Other residues make smaller contributions, but their cumulative effect is important; e.g., Asn-10, which is near DHAP (the NH_2 group is 3.1 Å from O1 of PGH in the crystal) contributes 2.6 kcal/mol to step a → b in Figure 1A. Figure 2 shows that a number of residues rather far from the active site have a significant effect on the ability of the enzyme to facilitate the reactions, although there could be some reduction in the contribution of the more distant residues by dielectric shielding that is not fully accounted for in the stochastic boundary simulation. Examples are Glu-97 and Lys-237 for reaction a → b and Arg-98 and Arg-99 for reaction b → c; as expected, the effect of the two arginines is smaller for the reaction with His-95 protonated (≈10 kcal; not shown) than unprotonated (14 kcal). That all the significant residues are conserved[1] suggests fine tuning of the reaction by appropriate selection of charged residues in evolution.

DISCUSSION

To obtain a clearer understanding of the catalytic mechanism, we consider the first reaction step (Glu⁻ + DHAP → GluH + enediolate) in some detail; the calculated energetics are given in Figure 4. Although analyses of enzyme functions are usually made relative to the reaction in solution (Jencks, 1975), we considered the gas phase to show the full effect of the enzyme. Also, because Glu-165 undergoes a chemical change in the reaction, we include it explicitly in the energy evaluation. The calculated gas-phase energy difference between the separated reactants (Glu⁻ + DHAP versus GluH
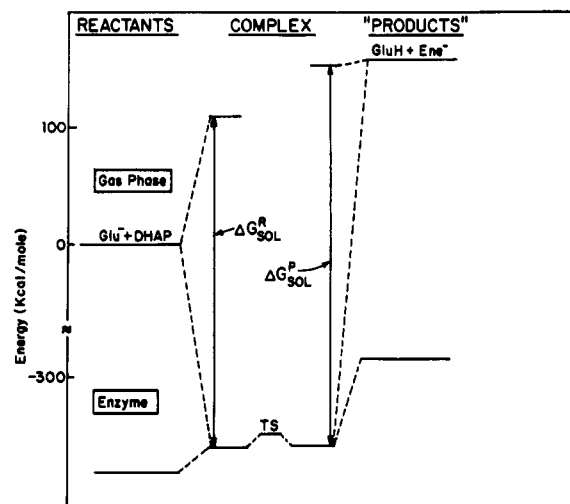

FIGURE 4: Relative energies for Glu⁻ + DHAP → GluH + Ene⁻. Gas-phase calculated values are shown for the separated reactants (taken as the zero of energy) and separated products and for the reactant complex and the product complex with structures corresponding to those in the enzyme. The gas-phase calculations are for $CH_3CH_2CO_2^-$ and $CH_3CH_2CO_2H$ as models for Glu⁻ and GluH. Corresponding values are shown in the enzyme; the separated reactant and product energies correspond to calculations with the other reactant (product) present but with the charges set to zero and so are approximations to the actual energy. The arrows designated ΔG^R_{SOL} and ΔG^P_{SOL} correspond to the stabilization of the enzyme–reactant [Glu⁻, DHAP] and enzyme–product [GluH,Ene⁻] complexes by interactions with the enzyme.

+ Ene⁻) equals ≈160 kcal. This is reduced to about 50 kcal simply by placing DHAP in the position it has, relative to Glu⁻, in the enzyme–substrate complex. DHAP and Glu⁻-165 are strongly destabilized by their interactions because both are negative ions, while for the enediolate and neutral GluH-165, the interaction energy is small. Thus, the proximity of the

Accelerated Publications

Biochemistry, Vol. 30, No. 24, 1991 5831

reactants resulting from binding of the substrate alters not only the entropy (Kraut, 1988) but also the energy of the reaction. The importance of such "ground-state destabilization", in addition to transition-state stabilization (Jencks, 1987), has been pointed out (Jencks, 1975; Kraut, 1988; Belasco & Knowles, 1980), although it has been difficult to substantiate (Jencks, 1975; Kraut, 1988). Given the proximity, the role of the enzyme is to further equalize the energy of reactants and products while simultaneously lowering the transition-state barrier (Figures 1B and 4). Both reactant ions and the enediolate "product" are strongly stabilized by the enzyme (GluH is only weakly stabilized); the former are less stabilized than the latter because protein residues, such as Lys-12, have stronger interactions with the extra charge on the enediolate, relative to DHAP. The GluH–enediolate complex is stabilized relative to the gas phase by about 510 kcal (almost entirely the enediolate), while the Glu–DHAP complex is stabilized by about 460 kcal with significant contributions from both Glu⁻ and DHAP. Overall the enzyme energetics are more similar to the solution than the gas phase; e.g., the free energy difference between the noninteracting reactants (Glu⁻ + DHAP) and the noninteracting intermediates (GluH + Ene⁻) is about 160 kcal/mol in the gas phase and about 20 kcal in aqueous solution, as estimated from the pK_a differences for the various species. The values used are $pK_a = 4$ for GluH and $pK_a = 19$ for the methylene proton of DHAP; the latter is based on the experiments of Chiang et al. (1986). In the enzyme the effective pK_a of GluH and the methylene proton of DHAP are nearly balanced from the calculation. The ability of enzymes to alter pK_a values is well-known; e.g., the pK_a of a Lys residue in the enzyme acetoacetate decarboxylase, which is reduced by over 4 units by the presence of the positive charge on an adjacent Lys (Westheimer & Schmidt, 1955). Continuum electrostatic calculations illustrating this effect have been made for lysozyme (Bashford & Karplus, 1990).

From Figure 2 it is evident that the enzyme has opposite effects on the two steps of the reaction; i.e., the protein *stabilizes* the formation of the enediolate/glutamic acid product in the methylene proton transfer reaction, which is highly *endothermic* ($\approx$160 kcal) in the gas phase (Figure 4), and *destabilizes* the enediol/imidazolate product in the proton transfer to the carbonyl group, which is highly *exothermic* ($\approx$132 kcal for a neutral histidine) in the gas phase. Charged species present along the reaction path (whether as reactants, transition states, intermediates, or products) tend to have large stabilizing interactions with enzymes; in the present system involving multiply charged ions, the interaction energy is near 500 kcal, which is of the same order as the solvation energy in aqueous solution. Stabilization by an enzyme of a charged group is generally dominated by specific nearby charges, though more distant interactions (Figure 2) and the surrounding aqueous solvent also play a role. The proposal (Dewar & Storch, 1985) that enzymes function simply by desolvating the reaction (i.e., to approach the gas reaction) is clearly not applicable to TIM.

CONCLUSION

The present simulations, although approximate, provide insights into the details of the TIM mechanism at the atomic level. Of particular importance are the large "solvation" effects for the ions involved that make it possible for the enzyme to alter the free energy barrier to a reaction or the equilibrium between reactants and products by as much as 160 kcal, as appears to be true here for reaction a → b, and suggest that an enzyme might use an unusual ionization state to carry out a reaction, as for reaction b → d. It is hoped that some of the specific results can serve as a guide to experimental investigations. NMR experiments are in progress (J. R. Knowles, private communication) that are designed to determine the protonation state of His-95 in the active enzyme, and site-directed mutagenesis studies are being done to test the role of remote charged groups on catalysis (J. R. Knowles, private communication; J. R. Knowles, G. A. Petsko, and D. Ringe, private communication).

ACKNOWLEDGMENTS

We thank Stephen Blacklow, Jeremy Knowles, and Elizabeth Komives for helpful comments on the TIM mechanism and careful readings of the manuscript.

Registry No. TIM, 9023-78-3; His, 71-00-1; Lys, 56-87-1; Asp, 70-47-3; Glu, 56-86-0; Arg, 74-79-3; DHAP, 57-04-5; GAP, 591-57-1.

REFERENCES

Alagona, G., Desmeules, P., Ghio, C., & Kollman, P. A. (1984) *J. Am. Chem. Soc. 106*, 3623.
Alber, T., Banner, D. W., Bloomer, A. C., Petsko, G. A., Phillips, D., Rivers, P. S., & Wilson, I. A. (1981) *Philos. Trans. R. Soc. London, B 293*, 159.
Albery, W. J., & Knowles, J. R. (1976a) *Biochemistry 15*, 5627.
Albery, W. J., & Knowles, J. R. (1976b) *Biochemistry 15*, 5631.
Banner, D. W., Bloomer, A. C., Petsko, G. A., Phillips, D. C., Pogson, C. I., & Wilson, I. A. (1975) *Nature (London) 255*, 609.
Bash, P. A., Field, M. J., & Karplus, M. (1987) *J. Am. Chem. Soc. 109*, 8092.
Bashford, D., & Karplus, M. (1990) *Biochemistry 29*, 10219.
Belasco, J. G., & Knowles, J. R. (1980) *Biochemistry 19*, 472.
Brooks, B. R., Bruccoleri, R. E., Olafson, B. D., States, D. J., Swaminathan, S., & Karplus, M. (1983) *J. Comput. Chem. 4*, 187.
Brooks, C. L., III, & Karplus, M. (1989) *J. Mol. Biol. 208*, 159.
Brooks, C. L., III, Karplus, M., & Pettitt, B. M. (1988) *Proteins: A Theoretical Perspective of Dynamics, Structure, and Thermodynamics*, Advances in Chemical Physics LXXI, John Wiley & Sons, New York.
Browne, C. A., Campbell, I. D., Kiener, P. A., Phillips, D. C., Waley, S. G., & Wilson, I. A. (1976) *J. Mol. Biol. 100*, 319.
Chiang, Y., Kresge, A. J., & Tang, Y. S. (1986) *J. Am. Chem. Soc. 108*, 460.
Davenport, R. C., Bash, P. A., Seaton, B. A., Karplus, M., Petsko, G. A., & Ringe, D. (1991) *Biochemistry* (preceding paper in this issue).
de la Mare, S., Coulson, A. F. W., Knowles, J. R., Priddle, J. D., & Offord, R. E. (1972) *Biochem. J. 129*, 321.
Dewar, M. J. S., & Thiel, W. (1977) *J. Am. Chem. Soc. 99*, 4899.
Dewar, M. J. S., & Storch, D. M. (1985) *Proc. Natl. Acad. Sci. U.S.A. 82*, 2225.
Dewar, M. J. S., & Dieter, K. M. (1986) *J. Am. Chem. Soc. 108*, 8075.
Dewar, M. J. S., Zoebisch, E. G., Healy, E. A., & Stewart, J. J. P. (1985) *J. Am. Chem. Soc. 107*, 3902.
Fersht, A. (1985) *Enzyme Structure and Mechanism*, W. H. Freeman & Co., New York.
Field, M. J., Bash, P. A., & Karplus, M. (1990) *J. Comput. Chem. 11*, 700.
Gaussian 86 (1986) Carnegie Mellon Quantum Chemistry Publishing Unit, Pittsburgh, PA.
Hall, A., & Knowles, J. R. (1975) *Biochemistry 14*, 4348.

Biochemistry **1991**, *30*, 5832–5838

Hartman, F. C. (1970) *Biochem. Biophys. Res. Commun. 39*, 384.

Haspra, P., Sutter, A., & Wirz, J. (1979) *Angew. Chem., Int. Ed. Engl. 18*, 617.

Hehre, W. J., Random, L., Schleyer, P. v. R., & Pople, J. A. (1986) *Ab Initio Molecular Orbital Theory*, John Wiley & Sons, New York.

Herlihy, J. M., Maister, S. G., Albery, W. J., & Knowles, J. R. (1976) *Biochemistry 15*, 5607.

Jencks, W. P. (1975) *Adv. Enzymol. Relat. Areas Mol. Biol. 43*, 219.

Jencks, W. P. (1987) *Cold Spring Harbor Symp. Quant. Biol. 52*, 65.

Karplus, M., & Petsko, G. A. (1990) *Nature 347*, 631.

Knowles, J. R., & Albery, W. J. (1977) *Acc. Chem. Res. 10*, 105.

Komives, E. A., Chang, L. C., Lolis, E., Tilton, R. F., Petsko, G. A., & Knowles, J. R. (1991) *Biochemistry 30*, 3011.

Kraut, J. (1988) *Science 242*, 533.

Lolis, E., Alber, T. C., Davenport, R. C., Rose, D. R., Hartman, F. C., & Petsko, G. A. (1990) *Biochemistry 29*, 6609.

Meot-Ner, M. (1988) *J. Am. Chem. Soc. 110*, 3071.

Nickbarg, E. B., Davenport, R. C., Petsko, G. A., & Knowles, J. R. (1988) *Biochemistry 27*, 5948.

Pearson, R. G. (1986) *J. Am. Chem. Soc. 108*, 6109.

Richard, J. P. (1984) *J. Am. Chem. Soc. 106*, 4926.

Rose, I. A. (1962) *Brookhaven Symp. Biol. 15*, 293.

Roux, B., Yu, H.-A., & Karplus, M. (1990) *J. Phys. Chem. 94*, 4683–4688.

Schroeder, S., & Thiel, W. (1985) *J. Am. Chem. Soc. 107*, 4422.

Singh, U. C., & Kollman, P. A. (1986) *J. Comput. Chem. 7*, 718.

Waley, S. G., Mill, J. C., Rose, I. A., & O'Connell, E. L. (1970) *Nature (London) 227*, 181.

Wang, I. S. Y., & Karplus, M. (1973) *J. Am. Chem. Soc. 95*, 8160.

Warshel, A., & Levitt, M. (1976) *J. Mol. Biol. 103*, 227.

Westheimer, F. H., & Schmidt, D. E., Jr. (1971) *Biochemistry 10*, 1249.

Yegil, G. (1967) *Tetrahedron 23*, 2855.

Articles

Kinetic and Thermodynamic Characterization of the Interaction between Qβ-Replicase and Template RNA Molecules[†]

Martina Werner[‡]

Max-Planck-Institut für Biophysikalische Chemie, Postfach 2841, Am Fassberg, W-3400 Göttingen, Federal Republic of Germany

Received January 9, 1991; Revised Manuscript Received March 27, 1991

ABSTRACT: The specific binding of the RNA polymerase Qβ-replicase to some of its RNA template molecules, the single-stranded RNA variant MDV and also Qβ-RNA, was studied under various conditions by using a gel-retardation assay as well as filter retention. The dissociation of the replicase–RNA complex proceeds with first-order kinetics. The dependence of the dissociation rate constant on the concentration of monovalent ions suggests that there are three ionic contacts between the midivariant (MDV) RNA and the replicase. Through analysis of the temperature dependence of the dissociation rate constant, values of 35 and 43 kJ/mol were obtained for the activation energies of complex dissociation between Qβ-replicase and the minus (−) and plus (+) strands of MDV, respectively. The bimolecular association is of second order with high rate constants that increase when the temperature is raised and decrease at higher salt concentrations. The equilibrium constants vary between $4 \cdot 10^{11}$ M^{-1} and $5 \cdot 10^{7}$ M^{-1}, according to the reaction conditions. The temperature dependence of K_a gives $\Delta H = -39$ kJ/mol for MDV− and −47 kJ/mol for MDV+. Under nearly all conditions, distinct differences in the association and dissociation rates of plus and minus strands of MDV are observed. The binding of the small variant MDV to Qβ-replicase is three orders of magnitude stronger than the binding of the natural template Qβ-RNA.

Qβ-replicase is an RNA-dependent RNA polymerase that is synthesized during the infection of *Escherichia coli* cells with the phage Qβ. It specifically replicates the phage RNA and ignores the host RNA. In vitro, Qβ-replicase also multiplies some smaller single-stranded RNA molecules with a size in the range 30–220 nucleotides very efficiently. Some of these variants were generated in in vitro evolutionary experiments starting with Qβ-RNA (Mills et al., 1967). Others, the midi-, mini-, and nanovariants, were synthesized in vitro without the addition of an exogenous template (Kacian et al., 1972; Sumper & Luce, 1975; Mills et al., 1975; Schaffner et al., 1977). The 6S RNA was isolated from *E. coli* cells infected with Qβ-phages (Banerjee et al., 1969; Kacian et al., 1971). While Qβ-RNA and the midivariant RNA have a common sequence motif (Nishihara et al., 1983), most of the replicable RNA variants do not show sequence similarities. Most likely the replicase recognizes structural features. Biebricher et al.